SCIENCE AT THE ENVIRONMENTAL RESEARCH STATION SCHNEEFERNERHAUS/ ZUGSPITZE

Prof. Dr. Michael Bittner; Ed.
(Coordinator Science Team UFS)

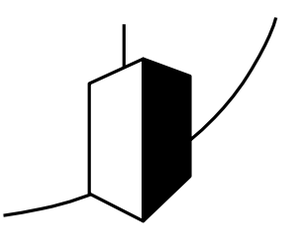

Umwelt
Forschungsstation
Schneefernerhaus

Table of contents

12 Evaluation of Measurement Series from high Mountain Stations

Ludwig Ries, Cedric Couret, German Environment Agency; Ye Yuan, Technical University of Munich; Esther Giemsa, Jucundus Jacobeit, Institute of Geography, University of Augsburg; Stephan Hachinger, Leibnitz Supercomputing Centre

12.1 Mountain Stations (Ludwig Ries)

12.1.1 The first alpine measurement stations and the present situation

The first high mountain stations were pioneers in atmospheric and climate research. In Central Europe, for example, important Alpine observation stations had been set up between the end of the 19th century and the first third of the 20th century. At a time when there were practically no methods of remote observation, these observatories enabled pioneering research to be carried out in the field of weather observation. Under very suitable visibility conditions, the radius of the observations could be extended to a range of more than 200 km. Apart from coastal areas, these weather stations were the first observatories for atmospheric remote sensing. As a result, it had become possible to detect weather changes at long distances and to transmit the results by telegraph to the central weather offices. In Austria, for example, the station Hoher Sonnblick was opened in 1886. The weather tower on the Zugspitze in Germany started in 1899 and the station Jungfraujoch in Switzerland in 1931. The station Puy de Dome in Auvergne, France, even had begun in 1876.

Since the mid-20th century, the number of high mountain stations worldwide has increased considerably. Today, a network of high mountain stations in Africa, Asia, North and South America supports atmospheric environmental monitoring and climate research. Even today, the great scientific advantage is the highly precise continuous measurement along the time axis.

12.1.2 Mountain stations in the Global Atmosphere Watch program

A prominent group of mountain stations supporting atmospheric research contributes to the station network of the Global Atmosphere Watch program (GAW). GAW started in 1989 as module for monitoring the physical and chemical state of the atmosphere within the Global Climate Observing System (GCOS) of UNO/WMO. From the very beginning the ground based, fixed station network had been the backbone of the Global Atmosphere Watch monitoring program. Presently GAW has evolved to an integrated network for atmospheric chemistry and physics observations, with additional ground based remote sensing measurements and measurements from ships, air planes and satellites.

The map (Fig. 1.1) provides the geographic distribution and the types of stations on mountains and selected high elevated sites, operating presently for atmospheric environmental research in GAW (cf. Tab. 1.1).

12.1.3 What is a mountain station?

In the sense of practical exploration, mountain stations provide platforms for atmospheric measurements at particularly representative locations on the mainland or on an island to allow drawing conclusions about the state of the atmosphere for a catchment area as large as possible. The amount of representative data in the measured time series should be as high as possible. This includes, that appropriate locations for mountain stations should be minimally influenced by pollution or other relevant anthropogenic influences.

12

Fig. 1.1: Map of GAW global observatories. GAW regional stations and contributing stations contribute for specialized atmospheric chemistry and physics monitoring supporting the worldwide Global Atmosphere Watch program. The selection includes stations which are in operational status and which measure aerosols and/or gases (greenhouse and reactive gases) and meteorological parameters. Data source: Gawsis station information system: https://gawsis.meteoswiss.ch

In contrary to the definitions of high mountain regions used in geography and geomorphology, we target an understanding, that applies worldwide across different climate zones and altitudes. In this way, for example, a comparable characteristic for lower altitude sites can be specified for moderate climates. However, this will not apply also to warmer climatic zones in South America or to highlands in largely uninhabited desert areas (e.g. Himalaya) or to areas in the Arctic and Antarctic. Considered worldwide, the characteristics cannot be understood as being constant over different climatic zones.

For a better comprehension of the whole phenomenon and because the characteristics for high mountain stations change fluently from higher to lower sites this text also refers partly to lower mountain sites. The overall objective of this chapter is, to identify the characteristics that high mountain stations and mountain stations in general have in common, to differentiate them and to be able to use these characteristics to analyze and understand measurement series from high mountain and mountain stations.

12.1.4 The objective of measurements at high altitude stations

The principal purpose for the measurement of high-altitude data is gaining representative information about the state of the atmosphere and the lower free troposphere. For example, for measurements for Global Atmosphere Watch, the main objective is to monitor the chemical and physical state of the atmosphere for detecting effects on climate change and to improve scientific understanding of the global climate system. This is different from the classical understanding of monitoring air quality which focuses on the adverse health effects on people from air pollution and which concentrates on ground-based sites in populated and additional at rural regions. Despite the very successful emergence of ground-based remote sensing programs measured time series from altitude mountain stations have the essential advantage to provide consecutive information along the time line. This enables a combined analysis. Remote sensing delivers data along the vertical altitude scale but mostly only for short times. Additionally, measuring the same parameter on a fixed mountain station, the monitoring data deliver a continuous time history along the time scale. A newer example for such a timeseries at Zugspitze station can be found in Yuan Y. and Ries L. et al., 2018. Together both kinds of data from both scales are essential for a better understanding and support validation and quality assurance of scientific results.

Tab. 1.1: Table of 45 GAW stations. It consists of global observatories, GAW regional stations and contributing stations working for additional monitoring activities supporting GAW. The selection includes stations which are in operational status and which measure aerosols and/or atmospheric gases (greenhouse and reactive) and meteorological parameters. Sites have been selected with altitudes starting from 950 meters a.s.l. or higher. Reference: Gawsis station information system: https://gawsis.meteoswiss.ch

WMO Region	Country	Station	Elevation (m a.s.l.)	GAW Station Type	Latitude (in °)	Longitude (in °)
Africa	Algeria	Assekrem	2710	GAW Global	23.26666641	5.633333206
Africa	Spain	Izana (Tenerife)	2373	GAW Global	28.30900002	–16.49939919
Africa	France	La Reunion	2160	GAW Regional	–21.0796	55.3841
Africa	Kenya	Mt. Kenya	3678	GAW Global	–0.0622	37.29719925
Antarctica	France	Concordia, Dome C	3233	GAW Other	–75.0998612	123.3334808
Antarctica	Belgium	Princess Elisabeth station	1350	GAW Regional	–71.95	23.35
Antarctica	United States	South Pole	2841	GAW Global	–89.9969482	–24.79999924
Asia	Taiwan, Province of China	Lulin	2862	GAW Other	23.46999931	120.8700027
Asia	China	Mt. Waliguan	3810	GAW Global	36.28749847	100.8963013
Asia	Nepal	Nepal Climate Observatory – Pyramid	5079	GAW Global	27.95779991	86.81490326
Asia	Viet Nam	Pha Din	1466	GAW Regional	21.5731	103.5157
Europe	Armenia	Amberd	2070	GAW Regional	40.38333511	44.25
Europe	Bulgaria	BEO Moussala	2925	GAW Regional	42.17919922	23.5855999
Europe	Slovakia	Chopok	2008	GAW Regional	48.96666718	19.60000038
Europe	Germany	Hohenpeissenberg	985	GAW Global	47.80149841	11.00961971
Europe	Switzerland	Jungfraujoch	3580	GAW Global	46.54748917	7.985089779
Europe	Russian Federation	Kislovodsk	2070	GAW Regional	43.72999954	42.65999985
Europe	Slovenia	Krvavec	1740	GAW Regional	46.29734948	14.53331438
Europe	Italy	Monte Cimone	2165	GAW Global	44.16666794	10.6833334
Europe	Italy	Monte Curcio	1796	GAW Regional	39.315972	16.42325
Europe	Spain	Montsec	1571	GAW Regional	42.051335	0.729564
Europe	Germany	Ochsenkopf	1185	GAW Other	50.0301	11.8084
Europe	Italy	Plateau Rosa	3480	GAW Regional	45.93534088	7.7073102
Europe	France	Puy de Dome	1465	GAW Global	45.7723	2.9658
Europe	Switzerland	Rigi	1031	GAW Regional	47.06739	8.46333
Europe	Germany	Schauinsland	1205	GAW Regional	47.90000153	7.916666508
Europe	Poland	Sniezka	1603	GAW Regional	50.73333359	15.73333359
Europe	Austria	Sonnblick	3106	GAW Global	47.05389023	12.95888901
Europe	Denmark	Summit	3238	GAW Regional	72.58000183	–38.47999954
Europe	Germany	Zugspitze-Gipfel	2962	GAW Global	47.421075	10.985896
Europe	Germany	Zugspitze-Schneefernerhaus	2671	GAW Global	47.4165	10.97964
North America	United States	Appalachian State University	1076	GAW Other	36.21300125	–81.69200134
North America	United States	Boulder Table Mountain (CO)	1689	GAW Other	40.125	–105.2369995
North America	United States)	Desert Rock (NV)	1007	GAW Other	36.61999893	–116.0179977
Central America	Mexico	Mex High Altitude Global Climate Observation Cente	4560	GAW Other	18.985842	–97.314433
North America	United States	Niwot Ridge – T-van (CO)	3523	GAW Regional	40.04999924	–105.5899963
North America	United States	Steamboat Springs (CO)	3220	GAW Regional	40.45500183	–106.7440033
North America	United States	Table Mountain (CA)	2286	GAW Regional	34.38233948	–117.688797
North America	United States	Wendover (UT)	1320	GAW Regional	39.90000153	–113.7200012
North America	Canada	Whistler Mountain	2182	GAW Regional	50.05929947	–122.9576035
South America	Bolivia	Chacaltaya	5340	GAW Regional	–16.2000008	–68.09999847
South America	Chile	El Tololo	2154	GAW Regional	–30.16833	–70.80361
South-West Pacific	United States	Mauna Kea (HI)	4204	GAW Other	19.82999992	–155.4799957
South-West Pacific	United States	Mauna Loa (HI)	3397	GAW Global	19.53623009	–155.5761566
South-West Pacific	Malaysia	Tanah Rata	1545	GAW Regional	4.484235	101.371606

12

12.1.5 What determines a site at high altitude?

12.1.5.1 Orography

For atmospheric research, it is not only the altitude above sea level that is relevant, but also the surface shape of the catchment area of the air masses which pass the station and whether the terrain is covered with vegetation and what the vegetation is like. It is also relevant how far away from the monitoring station there are settlement areas, how large the settlement areas are and what type and extent of air pollution is produced by the settlement areas. It is also crucial how the atmospheric circulation, which is determined by the climate zone and the surface shape in large, affects the transport of air masses to the measuring station, for example whether the station is situated on a coast or within a mountain chain or whether the mountain station is in the middle of a mainland or on an island, surrounded by the ocean.

Under special circumstances, an elevated station exceptionally may even not be located on a mountain. This is the case if the measuring station is located e.g., on an uninhabited plateau, which can be in a desert area or in a polar region. Examples for such stations are Assekrem (2710 m a.s.l.) in the Saharan region and South Pole (2841 m. a.s.l.). Despite the fact, that in this special situation the diurnal variation for determining representative periods of time and data must be interpreted principally different from sites on mountains, these stations were included also in this analysis. This was necessary, because on the one hand, the differences between the characteristics of the stations change fluently and it is relevant for a scientific understanding to analyze this situation correctly and to know the change of characteristics. And on the other hand, this knowledge is of fundamental importance when measurement series of elevated stations must be examined for their representativeness.

12.1.5.2 Meteorology

Apart from meteorological influences controlled by orography, mountain stations are exposed to continuously changing air masses from the atmospheric boundary layer and the lower free troposphere. This continuous change is controlled mainly by the diurnal variation and the seasonal variation. In moderate climates during the winter months from October to March mountain stations like site Zugspitze, are more frequently above the lower atmospheric boundary layer. Additionally, an existing snow cover then can prevent convective up wind transport. This results in a good separation from air within the atmospheric boundary layer (ABL) and clean air above. In contrast, during warmer summer and autumn a convective upwind system is formed, which transports during the day larger air masses from lower altitudes to the mountain station. Then often a maximum occurs in the midday and afternoon hours. In the evening hours the thermal upwind transport subsides again. The nightly cooling and collapse of the atmosphere causes that air masses with increased representativeness can be measured regularly at night. This thermal upwind phenomenon occurs when there is no snow cover under the influence of the sun on almost every mountain slope worldwide. In larger mountain regions, this intensive upward transport of air masses can lead also to an additional lateral horizontal transport of air. This phenomenon also is well known under the term alpine pumping. For further explanation see Winkler et. al. 2006.

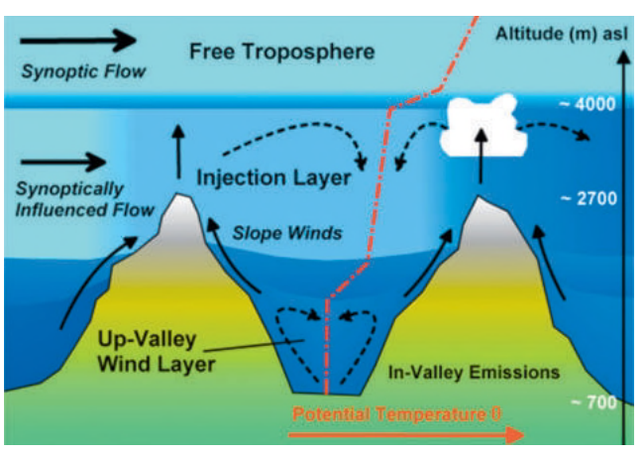

Fig. 1.2: Scheme of daytime air dynamics at mountain stations during summertime, according to Henne, 2004. For further explanation see the text.

Figure 1.2 presents a schematic overview about the daytime dynamics of air flow at high mountain stations in Europe. It shows synoptic flow as well as the mainly summerly thermic upwind system as well as the injection layer above, which contains especially during the season with long radiation length rests from the upward wind injection from the last day.

12.1.6 Spatial representativeness of mountain stations

The spatial representativeness of a measuring station is of fundamental importance for the significance of the measurement data and their interpretation. In this section, a selection of different approaches is presented to determine the spatial representativeness of an individual mountain station.

12.1.6.1 Contribution of the topography to the influence of the atmospheric boundary layer

Mountain stations receive continuous influences from the underlying ground in combination with the ongoing air mass transport. The surface structure of the surrounding topography impacts significantly the dynamics and hence measurable frequency and direction of air mass transport to the station. Collaud, 2018, identifies topographical features which influence aerosol measurements at high altitude stations. Due to the dominant effect of the individually pronounced topography it becomes evident that the station height alone is not always a sufficient criterion for predicting correctly the proportion of measurements in the lower free troposphere (LFT). This approach can be used to compare the potential representativeness between stations or for the planning and selection of an optimal new site location between several opportunities.

12.1.6.2 Analysis of regions of ground influenced wind origin by sector classification

With meteorological data transport modelling can be used to gain quantitative information about the representativeness of a station. The presented approach uses a geometrical analysis of the flow frequencies, classified in direction and distance from the measurement station. The result gives a classification of regions of origin of wind transported to the measurement site. In the following example for site Zugspitze Schneefernerhaus the transport model FLEXPART with backward directed dispersion trajectories has been applied to a longer and hence representative 2-year data set of meteorological analysis data. Around the original grid point of the Environmental Research Station Schneefernerhaus a set of circles has been constructed with radii 300 km, 600 km and 900 km. Additionally in each of the four main directions NW, SW, SE and NE the circles have been subdivided in rectangular sectors. Thus, the whole area consists of 12 circular segments. For the analysis of the station ground influenced wind data have been selected from cases when the wind before arrival had passed an altitude of maximal 150 m a.s.l. or below. The relative ratio of frequency of arriving ground influenced wind is defined as footprint signal and thus can be quantified as a function of the cardinal direction. The resulting frequency statistic shows the possible ground influence from on-flowing wind which can affect measurements at the station. These frequency statistics explain the numerically complex results in a simpler and better communicable form. The analysis was only carried out with a maximum transport time of 5 days for European wide calculations. For each region, the percentage share of the total footprint sum was calculated in the model domain Europe. The area of this model domain ranged from 75 to 35 °N and from –10 °W to 34 °E (Fig. 2).

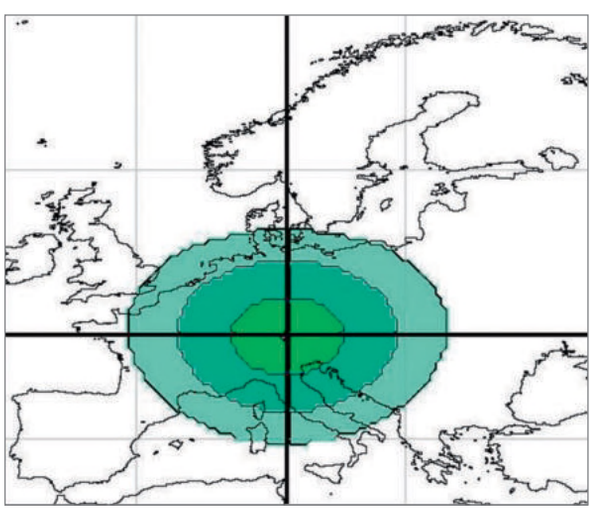

Fig. 1.3: Geometrical scheme of the 12 sectors around the site Environmental Research Station Zugspitze/Schneefernerhaus. Source: Birmili et. al. 2008.

Tab. 1.2: Relative transport frequency of on-streaming wind to the Environmental Research Station Schneefernerhaus with a maximum transport time of 5 days. The data are from 2005 and 2006. Applied Transport model was FLEXPART. All releases from 00:00 to 24:00hr have been used. Source: Birmili et. al. 2008.

Radius (km)	NW (in %)	SW (in %)	SE (in %)	NE (in %)	Total (%)
300	5.50	19.93	3.38	4.91	
600	5.18	10.62	2.41	2.27	
900	3.95	5.89	1.89	1.83	
Sum	14.63 (%)	36.44 (%)	7.68 (%)	9.01 (%)	67.76 (%)

12

12.1.6.3 Station footprints as quantifiable areas of influence from arriving ground-based winds.

The atmospheric dynamic produces very differentiated transport patterns of air arriving at a mountain station. Air mass transport is a result of the continuously measured and varying weather events. To gain quantifiable information about direction and frequency of transported air a series of backward directed dispersion trajectories (retro-plumes) can be used systematically. The following example for the site of Zugspitze-Schneefernerhaus is based on the meteorological analysis data of two consecutive years. The FLEXPART transport model was used to calculate series of backward trajectories. The results are values of a source-receptor relationship (QRB) as a function of latitude, and length for a release time t. This QRB is defined to the length of stay in a 150-m high layer above ground ("footprint") The unit of the Footprint QRB is ns/kg. This can be interpreted as empirical frequency from where ground influenced air has arrived at the Environmental Research Station Schneefernerhaus within the time which was described by the given input data. Because of known seasonal variations in the atmospheric transport the integrated results show different characteristics for the integrated seasonal data.

During *wintertime* the influence from ground reaches a minimum. Reason is the better separation from the ground as result of the frequently quite lower atmospheric boundary layer during wintertime. Also, the influence of eastern transported air is minimal. Simultaneously the air mass transport from NW and W is increased, compared to the other seasons. This also can be seen in wind rose statistics, where during wintertime the highest windspeed from western directions can be observed.

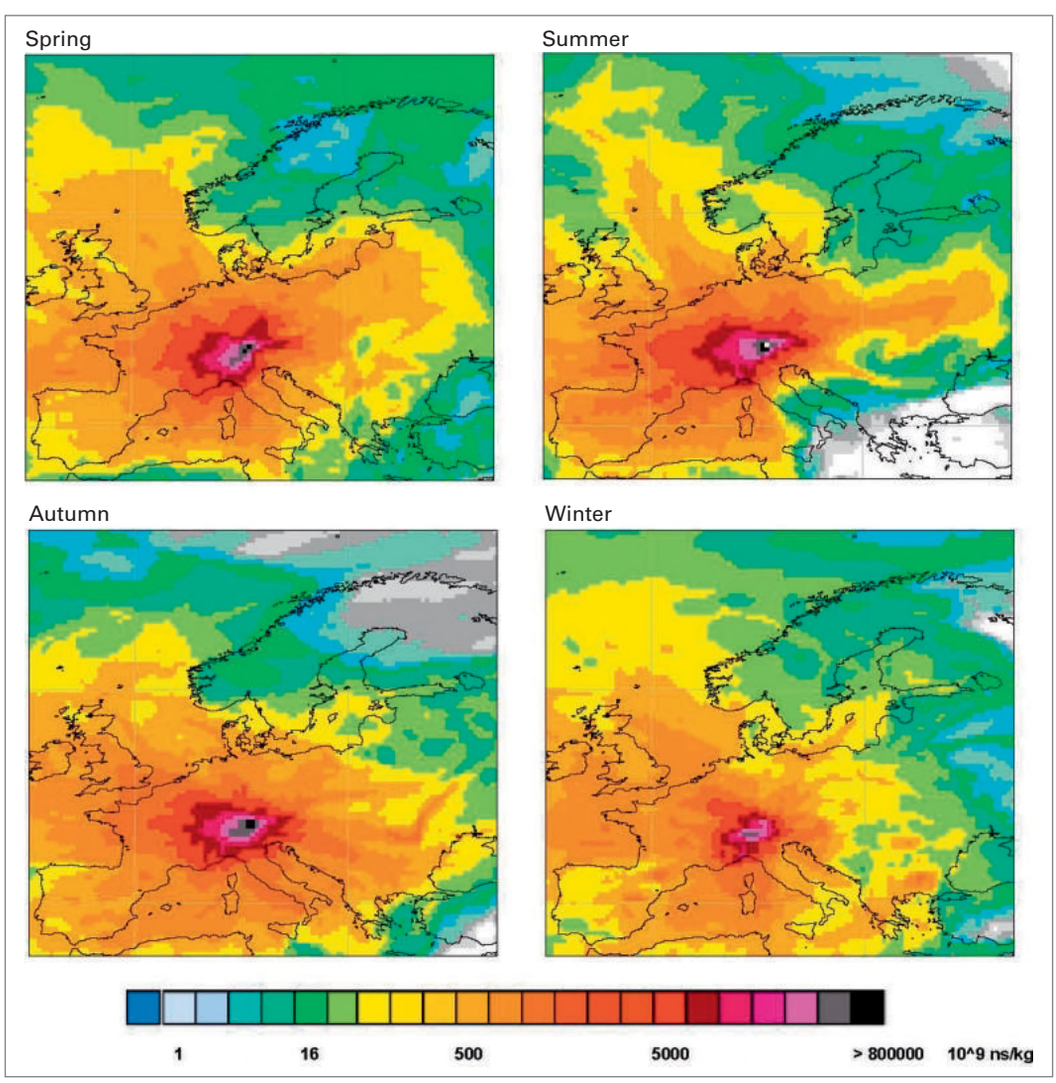

Fig. 1.4: Average seasonal transport frequency of air to station Zugspitze in the ground layer with a maximum transport time of five days for the duration of 2005 and 2006. Model: Flexpart, Source, Birmili et. al. 2008.

In *springtime*, the lateral wind transport and speed still is comparatively high. Like at wintertime conditions the lateral transport from western directions is enhanced. The convective upwind air mass transport starts and becomes gradually stronger with increasing day length.

At *summertime* the influence from ground-based air masses reaches a relative maximum. This can be understood as result of the intensive energy input from longer and more intensive sunshine duration and a resulting convective upwind system. This results in a more cellular weather regime and reduces long range lateral air mass transport mainly from western directions. During summer there is more eastern influence, whereas the western air mass transport changes from NW to W.

In *autumn*, the often-similar temperatures of the oceans and the continents create a more frequent stable air stratification. Because of relatively warm temperatures, compared to winter, the ground influence still is comparatively high.

12.2 Measurement series (Ludwig Ries, Cedric Couret)

Although the set of measurable variables in atmospheric chemistry and physics is much larger, in this section, we concentrate on selected measurement series examples from greenhouse gases, reactive gases and aerosols. The continuous measurement of parameters, relevant for the state of the Earth Atmosphere is a core issue in monitoring the changes in the climate system of the Earth's atmosphere. Within this section selected key measurement variables are presented being measured continuously by Global Atmosphere Watch for the Global Climate Observation System (GCOS).

12.2.1 Selected examples of measurement series and their role in atmospheric chemistry and physics

12.2.1.1 Carbon Dioxide

The most important cause of global warming are man-made greenhouse gases. Due to its high atmospheric concentrations, carbon dioxide is the most important greenhouse gas in addition to water vapor. The global concentrations of CO_2 have increased by 40 % since the beginning

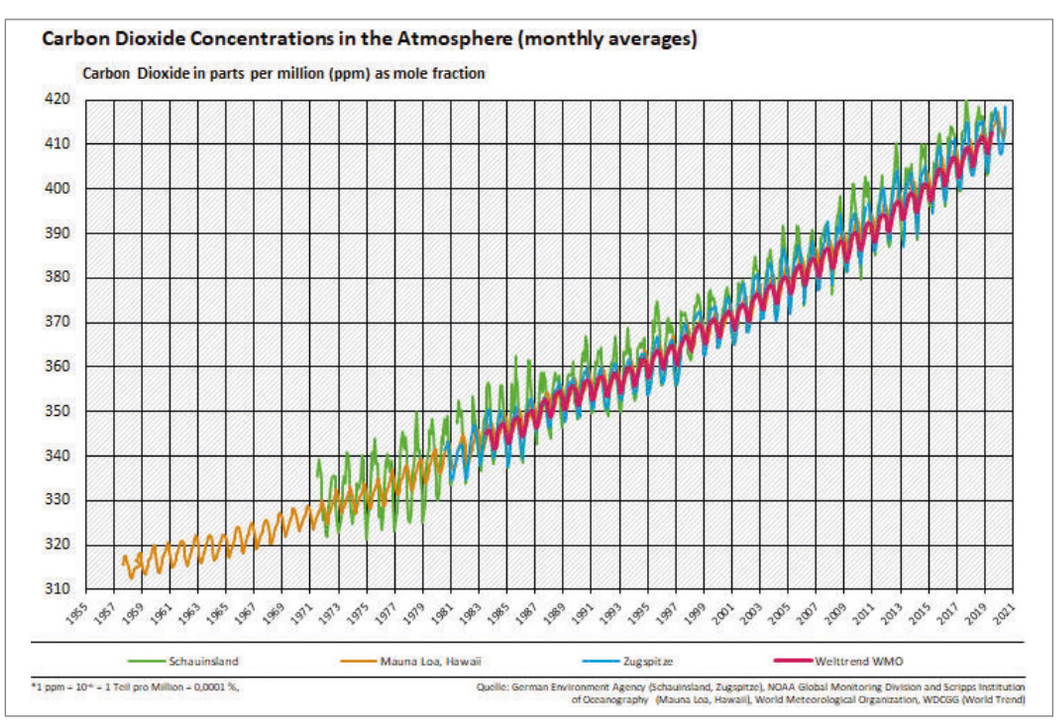

Fig. 2.1: Measured time series of carbon dioxide from Schauinsland GAW Regional station, Mauna Loa GAW global station and Zugspitze GAW global station, additionally compared with an average atmospheric CO_2 world trend. Source: website of Umweltbundesamt. www.uba.de

of industrialization in 1750. In contrast, CO_2 concentrations were almost constant in the previous 10000 years. The current increase in CO_2 is about 100 times faster than ever before in the past.

Long rows and their meaning

Long CO_2 measurement series provide a reliable measure of the global increase in CO_2 and continuously document the effect of fossil fuel combustion on the atmosphere. Thanks to their accuracy, they enable science to distinguish the effect of fossil fuel combustion from the seasonal fluctuation of the biosphere. This provides a reliable basis for analyzing long-term changes in the CO_2 reserves in the atmosphere with climate models and calculating future scenarios. Whereas in the 1950s the annual increase averaged 0.55 ppm CO_2 per year, differences in annual mean values over the past decade have shown an increase of about 1.9 ppm per year. Compared to the 1950s, global CO_2 production has thus more than tripled.

12.2.1.2 Methane

Since the pre-industrial age, the occurrence of methane (CH_4) in the atmosphere has risen by 270 % due to anthropogenic activities. In the group of long-lived greenhouse gases, methane makes the second largest contribution to global warming after carbon dioxide. Never in the past 650,000 years has there been such high concentrations in the Earth's atmosphere. Despite a slower increase since 1990 and a stagnation of the concentration at a high level until 2005, climate models are predicting an accelerated increase in methane with increasing warming. Since 2007, global networks and satellites have been observing an increased increase in methane.

Long rows and their meaning

High-precision long time series provide a reliable picture of the methane concentrations, which ultimately result from the interaction of all sources and sinks. Although the sources for methane are known, the trends of the sources and their interaction with the sinks cannot always be adequately explained: With the methane trend as a whole still rising, the increase in methane has decreased continuously over the last two and a half decades and the reasons for this continuous decrease and the resulting consequences for the future warming of the atmosphere are not yet understood sufficiently. Long and reliable time series are of fundamental importance here so that the interaction of sources and sinks can be adequately explained in the future.

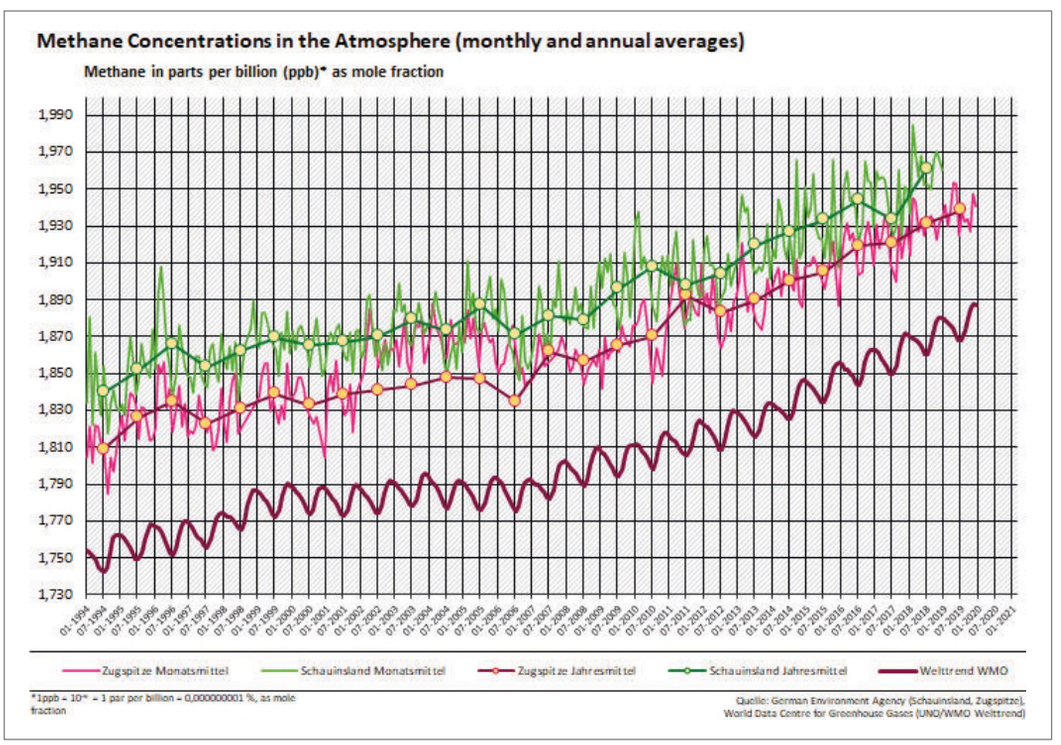

Fig. 2.2: Measured time series of methane from Schauinsland GAW Regional station and Zugspitze GAW global station, compared with the atmospheric WMO world trend, which shows lower concentrations, because it gives a more correct average over the whole earth surface (incl. oceans, which are no source area). Source: website of Umweltbundesamt. www.uba.de

12.2.1.3 Nitrous Oxide

Without their two most important representatives, CO_2 and CH_4, the long-lived greenhouse gases (LLCF) still account for a remarkably high proportion of the greenhouse effect. The most important are nitrous oxide (N_2O), sulphur hexafluoride (SF_6) and halogenated, climate-effective trace substances. In this group there are some substances with extremely long lifespan, such as SF_6 at 3200 years or NF_3 at approx. 640 years, which will continue to have still long-lasting impact on the global climate.

Long time series and their importance

Nitrous oxide makes the third largest contribution to global warming by long-lived greenhouse gases. Compared to the pre-industrial era (1750), its occurrence in the atmosphere has only increased by 20 %. But compared to CO_2, its influence on the warming of the atmosphere is 300 times stronger over a period of 100 years! Approximately 40 % of the N_2O emitted into the atmosphere comes from human activities. The rest comes from natural sources. The significantly higher percentage of land areas in the northern hemisphere and the use of artificial fertilizers in the mid-latitudes are the main reason for a small north-south gradient of nitrous oxide concentrations in the atmosphere. High-precision and long-time series in the northern and southern hemisphere are an important basis for a better understanding and forecasting of the temporal development of the sources. For this purpose, the in-situ measurement series must be measured with a very high accuracy of only 0.03 %. This meets the limit of the current technical feasibility.

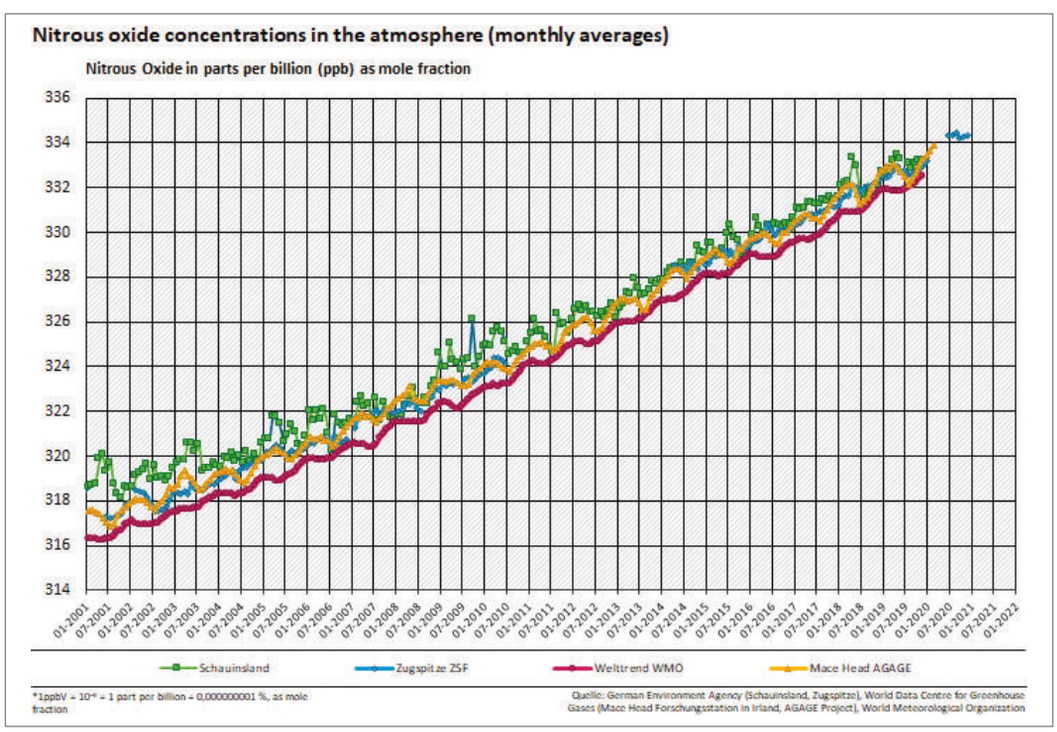

Fig. 2.3: Measured time series of nitrous oxide from Schauinsland GAW Regional station, Mace Head GAW global station and Zugspitze GAW global station and from WDCGG world trend.

12.2.1.4 Tropospheric Ozone

Ozone or trioxygen with chemical formula O_3 is a colorless gas, toxic for plants, animals, and humans. It plays a special role in the chemistry and physics of the Earth's atmosphere. Firstly, ozone is a greenhouse gas with a radiative forcing of approximately 0.4 W/m^2 (IPCC 5.th assessment report, 2013) which is approximately as large as the combined effect of all halogenated greenhouse trace gases. Then ozone is also a highly reactive gas, which plays an important role in the chemical transformation of likewise reactive nitrogen oxides in the troposphere. It should also be mentioned that the air layers above 10 kilometers contain over 90 % of the gas and that this stratospheric ozone absorbs most of the harmful ultraviolet solar radiation, which is an important prerequisite for biological life on this planet. In the following, however, only the tropospheric ozone will be considered.

Unlike in conurbations and cities where the atmospheric lifetime of ozone is significantly less than one day, ozone can have a lifetime of up to 3½ weeks in the much cleaner air at 3000 m altitude. As a result, ozone can be transported from North America, for example, and in some cases as far as from Asia to Central Europe in higher layers of air. Furthermore, additional ozone is formed photo-chemically in the troposphere from natural and anthropogenic ozone precursors, such as various VOCs or nitrogen oxides such as NO_2, by the action of sunlight.

Long continuous measurement series make it possible to combine short-term ozone measurements with a continuous history measured at a fixed location in the lower free troposphere. Thus they contribute to the plausibility check and quality control of remote sensing measurements. Several long measurement series of different measuring stations in a region enable parallel comparison and the validation of the temporal history of the development of atmospheric trends. This is also an important instrument for detecting errors in long-term measurement series. Furthermore, high-precision data representative of the lower free troposphere are an essential prerequisite for the ground calibration of satellite data over mainland. Only a highly time-resolved and highly precise measurement makes it possible to identify representative values that are unaffected locally and regionally.

The selected example of ozone measurements at the Zugspitze station shows at least the atmospheric result of two environmental protection measures. On the one hand, the discontinuation of the increase in ozone levels from 1983 shows the effect of the exhaust gas catalyst introduced in Germany and Central Europe at that time. The further decline in ozone background values from 2008 shows an effect of the success of the European environmental policy for the large-scale reduction of ozone precursors. See Bach H. et al. 2014, Ecorys.

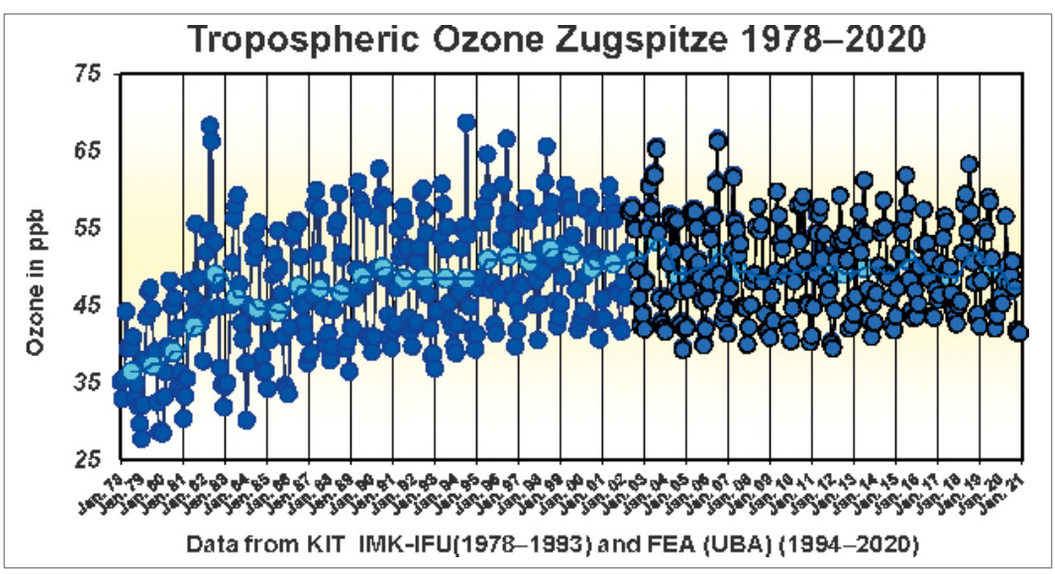

Fig. 2.4: Measured time series of ozone from Zugspitze GAW global station, measured with UV absorption photometer. From 1978 to 2000 data have been measured at Zugspitze summit station. Since 2001 the data are from Environmental Research Station Zugspitze Schneefernerhaus. The Schneefernerhaus data have been adjusted to the ozone level of the summit station. According to the + 0.82ppb O_3 long-time offset published with the station audit from 2011.

12.2.1.5 Aerosols

Aerosols have a largely cooling effect on the climate. Excluded from this is black carbon (BC) or soot, which belongs to the short-lived global warmers (SLCF). Situated on snow or ice, it reduces the backscattering up only to a few percent and thus has a strongly warming effect. However, black carbon in the atmosphere, heats the air masses but cools the underlying area on the ground. The mechanisms of climate warming effects of aerosols are not as well researched as with greenhouse gases. Also, the available measurement series of aerosols are significantly shorter than existing time series of greenhouse gases. An important known source of black carbon is traffic exhaust fumes, especially from diesel vehicles. Significant differences can be observed between high mountain sites (Zugspitze: 0.02 $\mu m/m^3$ annual mean value), rural sites (0.5 $\mu g/m^3$ annual mean value) and traffic influenced measurement sites with mean values around 2–4 $\mu g/m^3$.

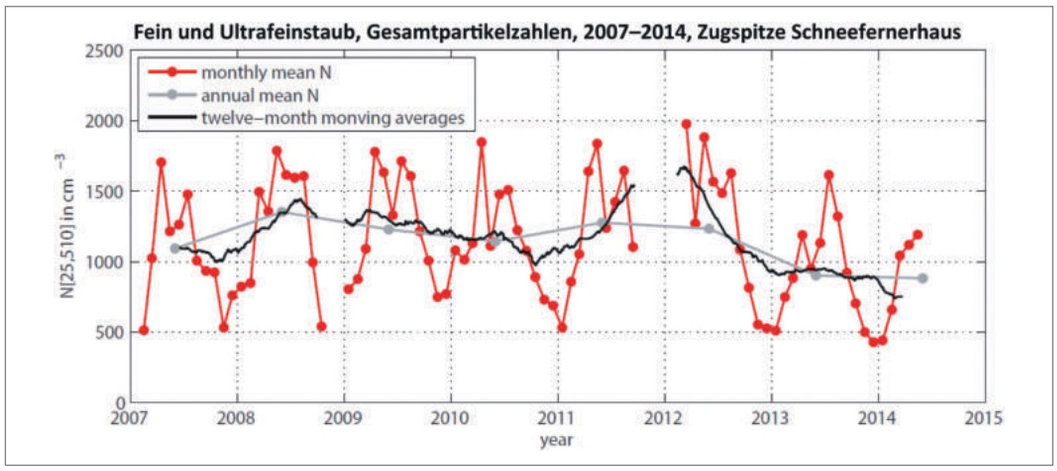

Fig. 2.5: Measured time series of fine and ultra-fine aerosols rom Zugspitze GAW global station, measured with scanning mobility particle sizer (SMPS) and condensation particle counter.

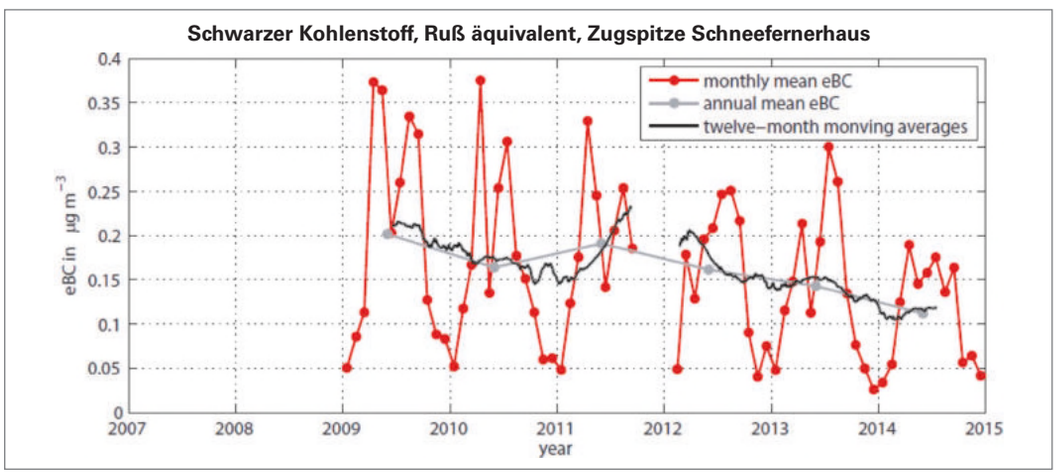

Fig. 2.6: Measured time series of atmospheric black carbon equivalent or soot (BC equiv.), measured with a multi angle absorption photometer (MAAP).

Like black carbon, ultrafine particles are a sensitive indicator of the influence of local combustion sources at a measurement site. A pronounced annual variation is observed for soot and fine and ultrafine particles. In winter, the highest readings occur in the lowlands. However, maximum concentrations are measured at the mountain stations in summer. The reason for this is the seasonal fluctuation of the mixing layer height. In summer the mixed layer is higher. In Central Europe, for example, its upper limit can be well over 3.5 km. This leads to good mixing during summer and relatively similar measured values of around 0.5 µg/m^3 at all rural measuring points located within the mixing layer. But in winter inversion layers become effective, which reduce the dispersion and increase the concentrations in the lowlands. During wintertime, mountain stations often are above these inversion layers and therefore then detect significantly lower concentrations.

In central Europe and on Environmental Research Station Zugspitze a declining trend could be observed since the beginning of the black carbon measurements in 2008.

12.2.2 Measurement techniques and quality objectives

Over the past decades, measurement technology and quality assurance have been continuously developed further and have led to a high level of development in the present. Since a more detailed treatment of the measurement technology and quality assurance procedures currently applied according to the state of science is beyond the scope of this chapter, the official sources of measurement technology and quality assurance in GAW are only briefly discussed here. The state of knowledge in GAW with recommendations for measurement technology and measurement quality assurance is described in the GAW technical reports of WMO. It can be accessed from https://library.wmo.int/

Because the objective of GAW is to generate a world-wide database for global analysis using comparable high precision and high-quality data according to the state of science, the consideration of data quality objectives and a consistent data preparation as elementary prerequisite for a coherent data quality is absolutely essential for the evaluation of measurement series.

12.2.3 Assurance of data quality

This short section is intended to help the scientific user of measurement series to know the necessary prerequisites for data quality to ask the right questions when selecting the data.

Scientific analysis requires data quality that meets the specified data quality objectives. For example, for the compatibility of greenhouse gas measurements in the Global Atmosphere Watch Program of the UNO/WMO, the quality targets are specified in the GAW Report No. 229 on page three. These quality objectives are an integral part of the measurement program and must be considered, when selecting the measuring instruments, carrying out the calibrations and the scale connections, as well as during the comparison measurements and evaluation of the calibrations.

The user of measurement data series must be aware that the production process of the data corresponds to a quality chain that is only as good as the weakest link. Scientific evaluations require data obtained under correct and always controlled conditions. In practice, almost every measured variable has special requirements, which must then also be considered correctly in the measurement experiment. For scientific evaluation, series of measurements must be used which have been correctly calibrated and which do not show a sudden shift in the value level over time, whose values have been viewed and checked over time and whose values lie on the current measurement scale to be used for GAW. Incorrect data must be specially marked or flagged in the data of the measurement series. These include data failures, artifacts, calibrations, measurement comparisons and influences from known air pollutants. To maintain the principle of traceability, flagged data is not discarded, but only marked. The originally measured data series is thus retained. It is good scientific practice to flag the data in a differentiated way.

12.2.4 Availability of measurement series

For scientific analysis data on the GAW measurement series are available for free via the GAW World Data Centers on the following topics:

Tab. 2.1: Selected world data centers for Global Atmosphere Watch monitoring data for the physical and chemical state of the atmosphere. Source GAW website: https://public.wmo.int/en/programmes/global-atmosphere-watch-programme

Topic	Link
World Ozone and Ultraviolet Radiation Data Center	http://www.woudc.org/
World Radiation Data Center	http://wrdc.mgo.rssi.ru/
World Data Center for Greenhouse Gases	http://ds.data.jma.go.jp/gmd/wdcgg/
World Data Center for Aerosols	http://www.gaw-wdca.org/
World Data Center for Aerosols	http://www.wdcpc.org/
World Data Center for Remote Sensing of the Atmosphere	http://wdc.dlr.de/

12.3 Analysis of the variation over time in measurement series (Ludwig Ries, Ye Yuan)

The central purpose for the measurement of high- altitude data is gaining more representative information about the state of the atmosphere in the lower free troposphere. Despite a systematically higher fraction of representative data at high altitude stations it is still a multifaceted scientific problem to differentiate less representative regional or locally influenced data from data which can be taken as representative.

On mountain sites atmospheric constituents show systematically different levels and variations in time, compared with other stations, situated in the lowlands or at conurbations. Often the levels of anthropogenic atmospheric pollutants are much lower at mountain stations. However, some other constituents like ozone show constantly higher levels.

No matter where and how the high-altitude measurements take place (continuous / discrete; in situ measurement/flask sampling), the measured data sets are usually treated as time series. Based on different measuring instruments and techniques, the measured time resolution could vary from seconds to days, weeks or even months.

For research and evaluation of data from measurement series from mountain stations the systematic analysis of the variation over time can be a very useful approach. Variations of data in time for example are diurnal, weekly, monthly, annual, or inter-annual variation. The following subsections explain some selected approaches more in detail.

12.3.1 Diurnal variation

Diurnal variation refers to the variation of data which had been measured during the day, by default from 0 a.m. local time (LT) this day to 0 a.m. local time the next day. The diurnal variation is very essential to understand and interpret short-term changes not only in atmospheric chemical constituents but also in physical and meteorological variables, such as temperature, aerosol concentration or solar radiation.

Practically at every measurement site a diurnal variation can be observed. But the characteristic of an individual diurnal variation is very specific for a site and hence decisive for the scientific interpretation and analysis of the measured data. In general, an analysis of diurnal variation requires data with 1 or ½ hr time resolution.

The figure 3.1 below presents four examples of the diurnal cycle from atmospheric CO_2 measured at high altitude site Zugspitze Schneefernerhaus. It shows a typical pattern for high elevated mountain stations during the four seasons. The CO_2 concentration levels remain relatively constant during a nightly time window, which is situated here at midnight. When the day starts with the morning hours, the CO_2 level increases by local influences and results in a diurnal peak by influence of air masses transported from local or regional sources.

Summertime: As the sun rises and starts with radiation, the lack of snow cover supports the development of anabatic winds, a daily thermal upwind system. Simultaneously, the upward transport of air with lower CO_2 levels caused by active photosynthesis reaches the measurement site. The up winds decrease until late night, when a nightly CO_2 level, more stable and with slightly higher values will be reached again. Then, after this minimum variation time window with especially well mixing the sun radiation of the next day starts again to build up the next thermic upwind system with upward transport of air masses. The intensity of this upwind system is driven by the duration of the sun radiation, which has its maximum on June 21st.

Wintertime: In wintertime generally, the nightly time window with especially well mixed air extends considerably longer. The driving factors then are the shorter length and weaker intensity of sun radiation and an existing snow cover, which suppresses the growth of a thermic

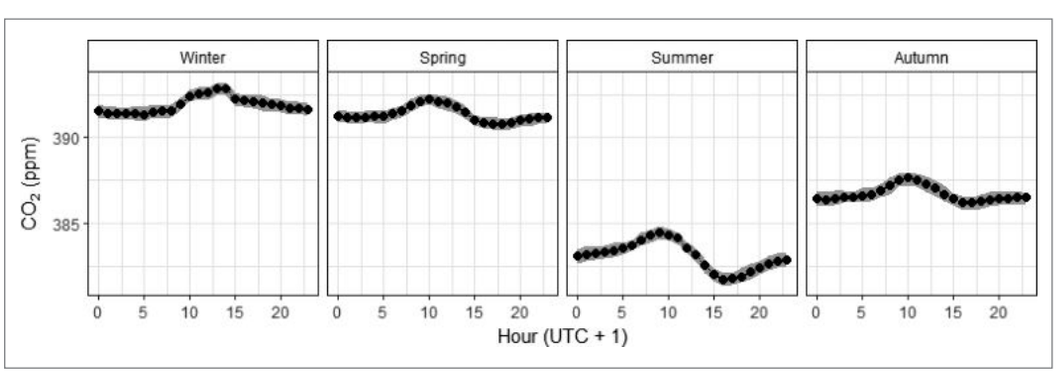

Fig. 3.1: CO_2 Mean CO_2 diurnal variations by season at measurement site Zugspitze Schneefernerhaus, Germany from 2002 to 2016. An explanation is given in the text.

12

upwind system. Often already at 21:00 h this nightly window starts and lasts considerably longer until to the morning hours of the next day at about 6:00 h. Under winter conditions at Zugspitze Schneefernerhaus a daily maximum builds up with a relative minimum during noon pause. In the average the winterly bimodal daily maximum follows the anthropogenic activity pattern on Zugspitze Platt.

At other mountain stations, the times of time windows can be different, being triggered by local orography and local to regional air mass transport, its current altitude and climate in connection with the geographic location.

12.3.2 Weekly variation

If the question is whether there is a regular systematic anthropogenic influence on the measurements in a time series, the investigation of the weekly variation can be a suitable approach to get to the root of this phenomenon. A week course of CO_2 measurements can hardly be explained by natural variability.

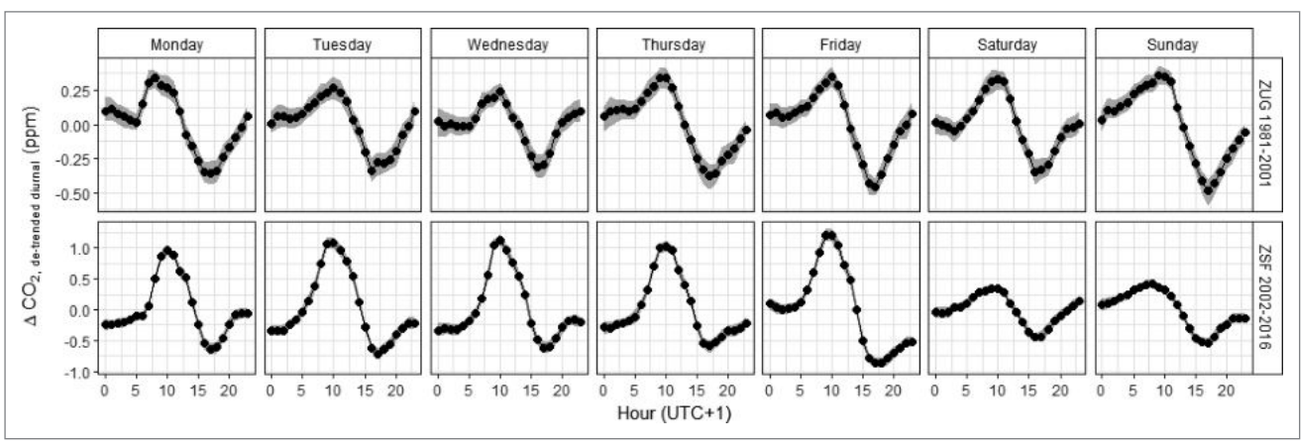

Fig. 3.2: Comparison of the weekly variation at two sites Zugspitze summit (ZUG, 1991–2001) and Zugspitze Schneefernerhaus (ZSF, 2002–2016). In contrary to the summit station at Environmental Research Station Schneefernerhaus a weekend minimum can be detected because the station is closed during weekends.

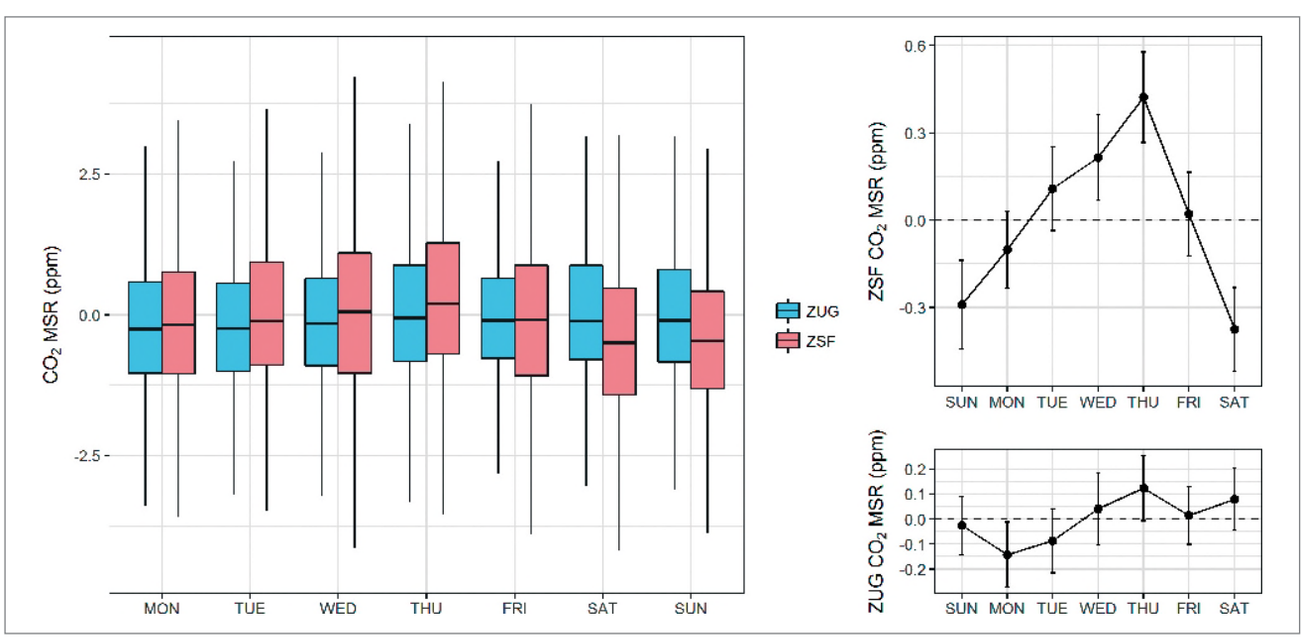

Fig. 3.3: Comparison of the weekly variation at two sites Zugspitze summit (ZUG) and Zugspitze Schneefernerhaus (ZSF). At Environmental Research Station Schneefernerhaus a weekend minimum can be detected in comparison to the weekly variation at Zugspitze summit. This is provided by the fact, that at weekends at site Schneefernerhaus there exists no anthropogenic activity, because of the closed station.

For example, the weekly variation between two sites can be displayed as a paired graphic comparison of seven mean daily courses, see Fig. 3.2. Depending on the problem, these daily courses can be averaged over the seasons of a year or several years, or they can be averaged over an entire year or over several years.

Another methodical approach for the analysis of weekly variations is the Mean Symmetrized Residual (MSR) statistic. The MSR can be regarded as a generalization of a residual over a weekly average. The calculation is described in Cerveny and Coakley, 2002, which tested this approach with CO_2 data on the Mauna Loa Station. The MSR retains the units of the measured variable and is directly comparable to atmospheric measured values. Furthermore, the method is robust enough for long-term trends and seasonal trends to have only a negligible effect on MSR statistics.

In Fig 3.3 the weekly variations at the two measuring sites Zugspitze Gipfel (ZUG) and Zugspitze Schneefernerhaus (ZSF) are compared. This comparison is displayed graphically as a pair of box plots of the MSR values or as a linear approximated week course, in which for each weekday an MSR value is plotted together with a ± 1-sigma uncertainty interval.

12.3.3 Annual variation

While the diurnal cycle itself can only provide information within relatively short time, an evaluation of the annual variation shows a more general view over the measured targets to track the seasonality and long-term trend. Annual variation can be calculated by differently aggregated data with interval length varying from hourly to monthly means. It is calculated by averaging the measured values into e.g. monthly averages to evaluate the variations between monthly values throughout the year. These variations are relevant due to biogenic activities which vary from season to season or the effect of the varying local transport dynamic during the different seasons.

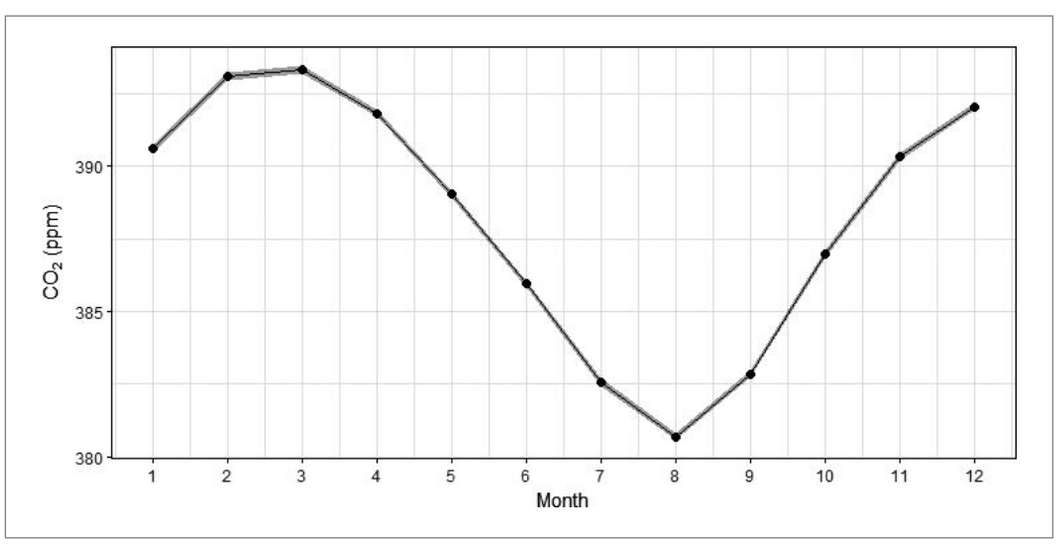

Fig. 3.4: Annual variation by monthly CO_2 averages from 2002 to 2016 at Zugspitze Schneefernerhaus, Germany.

From figure 3.4, we can see that there is a clear seasonal cycle of the atmospheric CO_2. The monthly maximum takes place in March and the minimum is in August. As the temperature rises from spring to summer, the effect of the photosynthesis of vegetation becomes increasingly stronger, causing the CO_2 levels to decline. When the vegetation growing season is over, the influence of photosynthesis to atmospheric CO_2 levels sinks and the CO_2 concentrations rise again. This explains the major cause for such seasonality in atmospheric CO_2 at high altitude measurement sites.

12.3.4 Case study example with Ozone, Carbon Monoxide and Nitrous Oxide

Gilge et al. (2010) compared long-term in situ measurements of atmospheric ozone, CO, and NO_2 at four alpine mountain stations in central Europe, which comprised Hohenpeissenberg and Zugspitze (Germany), Sonnblick (Austria), and Jungfraujoch (Switzerland). To give a general idea of the measurement results over time, the time series plots of all three components were represented by monthly mean values. The mean annual variations were plotted to explain the annual variation of the pollutants. The time series plots were also divided into four seasons with annual values for the comparison of different measurement sites in each season. Moreover, weekly variations (weekdays vs. weekend) were used to study whether there are working patterns during the week how they differ with data from weekend.

Regarding data analysis techniques, besides calculating the mean values, percentile was calculated for data analysis as well. By showing different range of percentiles (1^{st}/99^{th}; 5^{th}/95^{th}; 25^{th}/75^{th}) and minimum and maximum, the data quality and distribution with information of the outliers could be detected clearly. For trend estimation/approximation, linear regression with t-test, as one of the commonly used methods, was applied. In the following section, exemplary data analysis methods for evaluation of air mass transports and detection of pollution sources will be introduced.

12.4 Selection of representative data (Ye Yuan, Ludwig Ries)

12.4.1 Minimum diurnal variation

Atmospheric measurements are largely characterized by measurement sites. Within the Global Atmosphere Watch (GAW) network, two types of stations are defined with different research focuses as regional and global stations. One of the most essential goals at global stations is to detect the background level of atmospheric measurements. However, even though the global stations are mostly situated at remote areas, the measurements are still influenced by local to regional activities to certain extent. Therefore, to improve the data quality of the atmospheric measurements as well as the compatibility of measured data at different measurement sites, selection of the most representative is elementary.

Data selection is usually performed after data are obtained from measurement and have been validated. Data selection can be made based on various properties, such as meteorological parameters (wind speed, wind direction), chemical tracers (CO_2 vs. CO, CH_4) and statistical properties (data variability). The selected data represent the site-specific background values that form the basis for further analyses such as long-term trends, seasonality, influences of local sources and sinks, and comparison with satellite-based measurements.

In the following a newer statistical data selection method ADVS (Adaptive Diurnal Minimum Variation Selection) is presented in short. It was tested with atmospheric CO_2 measurements from 2010 to 2015 at six European elevated mountain stations (Yuan et al., 2018). The underlying automated algorithm selects data under best possible baseline conditions. It is based on the evaluation of the statistical structure of the given diurnal variation. As mentioned in Section 3.1, the diurnal variation alters seasonally, showing patterns resulting from different meteorological conditions, which are either from the lower free troposphere, or are influenced from local to regional sources. ADVS first detects a contiguous time window that has the least variation during the course of the day. Thereafter, the method starts the data selection based on the specified daily time window and examines the selection from the rest of the daily data based on statistical criteria. The figure 4.1 shows an example of selected atmospheric CO_2 data at measurement site Zugspitze Schneefernerhaus from 2002 to 2016. The advantage of the ADVS method is, that the selected data are remarkably close to the conditions of the lower free troposphere and that for central European stations the correlation between the stations is better than with several other compared selection methods. The disadvantage is, that the percentage of data, which have been detected is comparatively small. Practical experience has shown that the method also can be applied to atmospheric ozone and aerosol data.

12.4.1.1 Analysis of a 36-year time CO_2 measurement time series at mount Zugspitze

After initial standardization, the ADVS data selection could be applied subsequently to the entire existing measurement series. This was possible because the selection methodology exploits the inherent structural properties of the measured time series. In that way a selection of representative data also can be applied to past data time series. The resulting CO_2 trend and seasonality after the data selection and a decomposition of the long-term time series into trend and seasonal components resulted in a mean CO_2 annual growth rate over the 36-year period at Zugspitze is 1.8 ± 0.4 ppm yr^{-1}, which was in good agreement with the US-American Mauna Loa station and global means from UNO/WMO.

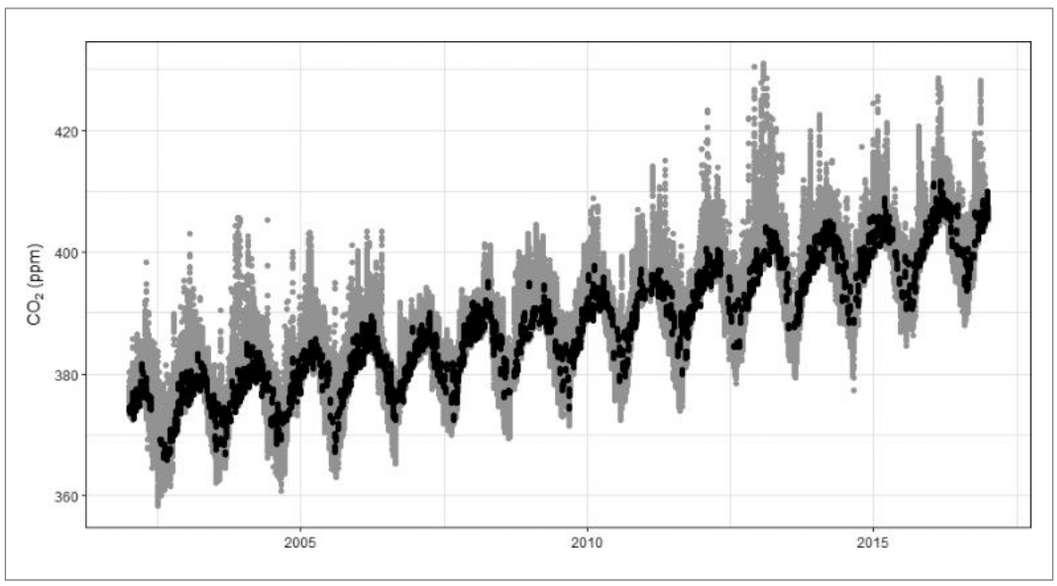

Fig. 4.1: Atmospheric CO_2 (in grey) from 2002 to 2016 at measurement site Zugspitze Schneefernerhaus with selected data (in black) by ADVS selection method.

12.4.1.2 Comparing selected CO_2 station measurement data with remote sensing and satellite data

The comparison of representative in-situ ground data with satellite data is of essential necessity for calibration of satellite measurements and required retrieval methods, especially over the continent. In 2019, Yuan et. al. showed a local comparison of in-situ CO_2 measurements at the Zugspitze site with co-located TCCON column measurements and results from satellite observations.

Based on the fact, that the application of consistent data processing routines to these CO_2 data with appropriate data preparation (retrieval and gap interpolation) is essential for a correct comparison of measurement results, trend and seasonality can be well extracted from all measurement datasets.

While the mean annual growth rates agreed well with about 2.2 ppm yr^{-1} over a 17-year period (2002–2018), the mean seasonal amplitudes showed significant differences (surface: 11.7 ppm/ column-averaged: 6.6 ppm), which could be attributed to different air masses.

The applicability of consistent data processing routines remains challenging, yet at the same time it is an essential necessity to ensure global comparability of highly accurate and high-quality atmospheric measurement data.

12

12.4.2 Ambient Radon concentrations as tracer for ground-based air

When ^{222}Radon is measured additionally at a measuring station, such data can be used for a selection of representative data. Radon provides a good approximation of ground influence. ^{222}Rn is an indirect decay product of the radioactive decay series of uranium or thorium and is produced in the bedrock below the mountain massif. The gas has a radioactive half-life of 3.8 days. In combination with meteorological data, radon measurements support the classification of air masses and are therefore also an essential prerequisite for more precise dispersion calculations and source allocations of gases and aerosols. Increased radon concentrations are an important criterion for distinguishing between ground-level, unrepresentative air masses and mountain air of the lower free troposphere, which is defined by low radon concentrations. Previous investigations show that a maximum atmospheric concentration of 1–2 Bq/m^3 ^{222}Rn at standard temperature and pressure is suitable as a criterion for unaffected mountain air. See also the work of Griffiths et al. 2014.

Compared to data selection with the minimum diurnal variation in 4.1, this method has the disadvantage that an additional measured variable must be measured but has the advantage of greater data yield. However, there is a possible restriction that the data selected as representative can nevertheless be influenced by regional or local sources from altitude sources, which may have to be additionally excluded.

References

Birmili, W., et al., Determining the northern hemispheric background at the GAW station Zugspitze under consideration of remote transport of fine airborne particulates. Research Report from UFOPLAN 204 42 202/01 (in German), 2008

Cerveny, R. S., Coakley, K. J., A weekly cycle in atmospheric carbon dioxide, (2002), Geophysical Research Letters, Vol 29, No. 2, pp. 15-1–15-4, doi = 10.1029/2001GL013952

Hanne Bach, Jørgen Brandt, Jesper H. Christensen, Thomas Ellermann, Camilla Geels, Ole Hertel, Andreas Massling, Helle Ørsted Nielsen, Ole-Kenneth Nielsen, Claus Nordstrøm, Jacob K. Nøjgaard, and Henrik Skov, *DCE – Danish Centre for Environment and Energy, Aarhus University (AU), Denmark,* Tim Chatterton, Enda Hayes, Jo Barnes, Duncan Laxen, Jimi Irwin and Jim Longhurst, *University of the West of England (UWE), Bristol,* Florent Pelsy and Tony Zamparutti, *Milieu, Belgium.* Services to assess the reasons for non-compliance of ozone target value set by Directive 2008/50/EC and potential for air quality improvements in relation to ozone pollution (Final report) assess the), Ecorys, Rotterdam, NL, 21. January 2014, for client: DG Environment. www.ecorys.nl, http://ec.europa.eu/environment/air/pdf/Final_ozone_report.pdf
(Quelle: Ufoplan Bericht des IFT Leipzig 3703 43 200 vom September 2011).

Henne S., Furger, M. Nyeki, S. Steinbacher, M., Neininger, B., De Wekker, S. F. J., et al. (2004). Quantification of topographic venting of boundary layer air to the free troposphere. Atmos. Chem. Pahys. 4, 497–509. Doi: 10.51.94/acp-4-497-2004

Hermann, W., Sun. J., Birmili, W. (2017) VAOII Projekt, Teilprojekt: TP I/02 Trends klimawirksamer Gase und Aerosole und raumzeitliche Deposition persistenter organischer Umweltschadstoffe – Unterteilprojekt 3: Erweiterte Untersuchungen zu klimawirksamen Aerosolen, Leibniz-Institut für Troposphärenforschung (TROPOS), 2017, Leipzig, 28 S.

Kürbis I. Fuzzy-Logic Filter für das Global Atmosphere Watch Programm. Entwicklung von datenbankgestützten Filterfunktionen zur Kennzeichnung der Luftmassen-Einflüsse in den Messreihen der Globalstation Zugspitze, Dissertation, Fakultät für Geowissenschaften der Ruhr-Universität Bochum, 2004 (Fuzzy Logic Filter for the Global Atmosphere Watch Programme. Development of database-supported filter functions for labelling the air mass influences in the measurement series of the Zugspitze Global Station, Dissertation, Faculty of Geosciences, Ruhr University Bochum, 2004. In German)

Collaud C., Andrews E., Aliaga D., et al. Identification of topographic features influencing aerosol observations at high altitude stations, August 2018, Atmospheric Chemistry and Physics 18(16): 12289–12313, DOI: 10.5194/acp-18-122892018

GAW Report No. 229, 18th WMO/IAEA Meeting on Carbon Dioxide, Other Greenhouse Gases and Related Tracers Measurement Techniques (GGMT-2015), La Jolla, CA, USA, 13–17 September 2015, Page 3. https://library.wmo.int/opac/doc_num.php?explnum_id=3074

Griffiths, A. D., Conen, F., Weingartner, E., Zimmermann, L., Chambers, S. D., Williams, A. G., and Steinbacher, M.: Surface-to-mountaintop transport characterised by radon observations at the Jungfraujoch, Atmos. Chem. Phys., 14, 12763–12779, https://doi.org/10.5194/acp-14-12763-2014, 2014.

IPCC, 2013: Climate Change 2013: The Physical Science Basis. Contribution of Working Group I to the Fifth Assessment Report of the Intergovernmental Panel on Climate Change [Stocker, T. F., D. Qin, G.-K. Plattner, M. Tignor, S. K. Allen, J. Boschung, A. Nauels, Y. Xia, V. Bex and P. M. Midgley (eds.)]. Cambridge University Press, Cambridge, United Kingdom and New York, NY, USA, 1535 pp,

Gilge S., Plass-Duelmer C., Fricke W., Kaiser A., Ries L., Buchmann B., Steinbacher M., 2010. Ozone, carbon monoxide and nitrogen oxides time series at four alpine GAW mountain stations in central Europe. Atmos. Chem. Phys. 10 (24), 12295–12316. 10.5194/acp-10-12295-2010.

Sigmund A., Freier K., Rehm T., Ries I., Schunk C., Menzel A., Thomas C. K., Multivariate statistical air mass discrimination for the high-alpine observatory at the Zugspitze mountain, Germany. April 2019, Atmospheric Chemistry and Physics, DOI: 10.5194/acp-2019-211

Winkler P., Lugauer M., Reitebuch O., Alpine Pumping, in Promet, Vol 32, Nr. 1/2, pp. 34–32 (in German), German Weather Service, 2006.

Yuan Y., Ries L., Petermeier H., Steinbacher M., Gómez-Peláez A. J., Leuenberger M. C., Schumacher M., Trickl T., Couret C., Meinhardt F., and Menzel A.: Adaptive selection of diurnal minimum variation: a statistical strategy to obtain representative atmospheric CO_2 data and its application to European elevated mountain stations, Atmospheric Measurement Techniques, 11, 1501–1514, https://doi.org/10.5194/amt-11-1501-2018, 2018. https://www.atmos-meas-tech.net/11/1501/2018/

Yuan Y., Ries L., Petermeier H., Trickl T., Leuchner M., Couret C., Sohmer R., Meinhard F., Menzel A. On the diurnal, weekly, seasonal cycles and annual trends in atmospheric CO_2 at Mount Zugspitze, Germany during 1981–2016, August 2018, Atmospheric Chemistry and Physics, DOI: 10.5194/acp2018-850

Yuan Y., Sussmann R., Rettinger M., Ries L., Petermeier H., Menzel A., Comparison of Continuous In-Situ CO2 Measurements with Co-Located Column-Averaged XCO2 TCCON/Satellite Observations and CarbonTracker Model Over the Zugspitze Region, Remote Sensing. 2019, 11, 2981; doi:10.3390/rs11242981

12.5 Analysis of transport and source contributions based on back trajectories (Esther Giemsa, Jucundus Jacobeit, Stephan Hachinger)

The chemical characteristics of an air mass are often closely related to the amount of time it has spent in close contact with surface-based sources and sinks in its recent history. To examine the contribution of emission sources and sinks to measured concentration levels, the pathways on which air masses have travelled can be recalculated using a Lagrangian particle and dispersion model and further analysed by so called receptor models. Receptor modelling approaches proceed from concentrations at a receptor site backward to responsible emission sources and sinks by relating the on-site arriving paths of air mass back trajectories to the simultaneously measured concentrations. Thus, the back-trajectory receptor models assess the air mass history to infer geographic regions with influence on the concentration levels at a particular measuring site (Hopke 2016, Cheng et al. 2015). Two of these source apportionment tools based on back trajectories are presented together with examples for their application to the CO_2 concentration measurements at the Environment Research Station Schneefernerhaus.

12.5.1 Back Trajectories

Air mass back trajectories as a result of dispersion and transport models provide an approximation of the path air parcels have recently covered thereby acquiring their observed characteristics (Crawford et al. 2009). Therefore, back trajectories act as a dependable tool for investigating dynamical processes in the atmosphere on synoptic time scales (Hopke 2016). Since they offer the possibility to identify the location of major emission sources and sinks, they have been widely used to infer geographic regions that contribute to pollution events, enabling detailed insights into source-receptor relationships within the catchment area of a given station (Cheng et al. 2015). Especially if many back trajectories (over months to years) are analysed in specific ways as described below, they identify the geographic origins mostly associated with concentration anomalies. With enough (dissimilar) trajectories, those locations leading to the measured concentration levels are revealed (Carslaw 2015).

To represent the chaotic pathways of air masses especially during their residence time in the turbulent planetary boundary layer as realistically as possible, Lagrangian Particle Dispersion Models (LPDM) compute trajectories of a large number of so-called particles (not necessarily

representing real particles, but infinitesimally small air parcels) to describe the transport and diffusion of tracers in the atmosphere (Fleming et al. 2012). The main advantage of Lagrangian models is that, unlike in Eulerian models, there is no numerical diffusion. Furthermore, in Eulerian models a tracer released from a point source is instantaneously mixed within a grid box, whereas Lagrangian models are independent of a computational grid and have, in principle, infinitesimally small spatial units (Stohl et al. 2002). Consequently, the Lagrangian box is assumed to behave like a point identically following the wind patterns (Seinfeld & Pandis 2016).

In our exemplary study carried out to investigate the contribution from emission sources and sinks to CO_2 concentrations measured at the Environment Research Station Schneefernerhaus, the LPDM FLEXPART (Stohl et al. 2005) was employed. For the traceability of the impact from sources and sinks through atmospheric transport and mixing conditions, a large ensemble of four-dimensional (three space dimensions plus time) ten-day back trajectories from the receptor site Schneefernerhaus every two hours over the entire study period 2000–2015 is calculated with the LPDM FLEXPART driven by the ERA-Interim analysis fields of the European Centre for Medium-Range Weather Forecasts (ECMWF) with 0.2° resolution. Based on the ECMWF meteorology fields, a total of 10 000 particles carrying the traits of CO_2 molecules were released every two hours over the entire study period and followed backward in time for ten days. The positions of the dispersing particles were stored with a 2-hourly time step. To reduce intrinsic model uncertainties such as the restricted resolution of the meteorological ECMWF fields and the parameterisations of the LPDM itself, the backward FLEXPART simulations of the particle dispersions are aggregated to their centroid tracks (red dashed line in Fig. 5.1) resulting in the cancelling-out of errors. As for the assumption that the uncertainties are equally distributed, the coordinates of the centroid tracks represent the mean, and thereby least erroneous, air mass transport path. The resulting centroid tracks of the particle dispersion form the basis for the further described back trajectory receptor models that relate variability in chemical observations – in our case: CO_2 concentrations measured at Schneefernerhaus – to variations in synoptic-scale circulations.

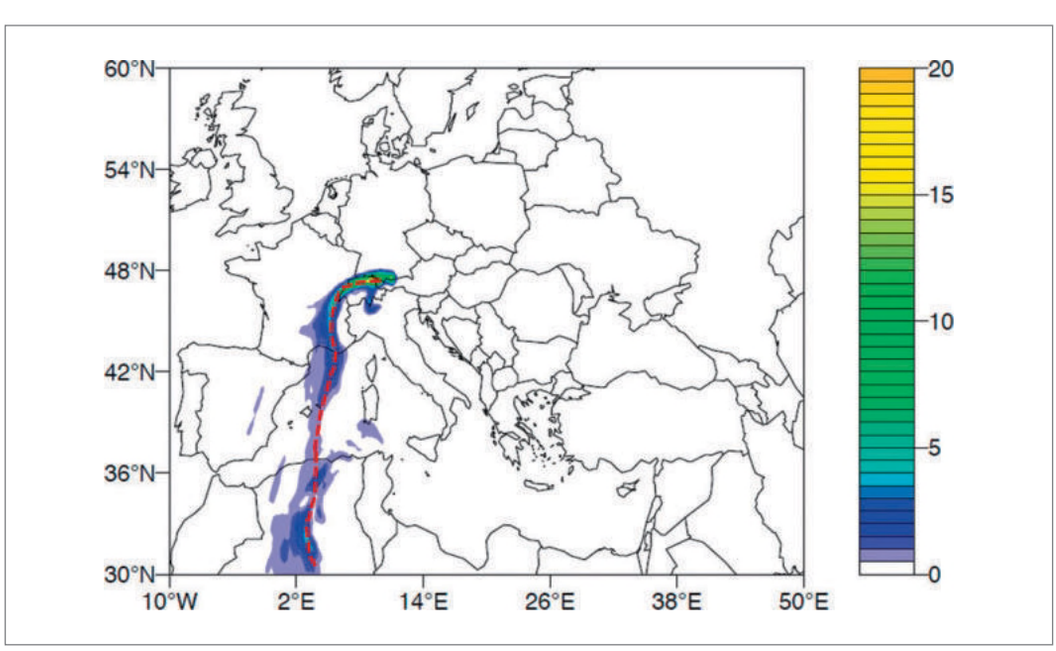

Fig. 5.1: Exemplary FLEXPART dispersion modelling [emission sensitivity in log(s/m^3/kg)] for 10 000 CO_2 particles released at the receptor site Schneefernerhaus backward in time together with the centroid track (red dashed line) corresponding to the mean transport locations of the particle tracing

12.5.2 Potential Source Contribution Function (PSCF)

The identification of geographic regions with impact on the CO_2 deviations at a particular site is performed by gridded receptor models based on air mass back trajectories. A well-known receptor model is the Potential Source Contribution Function (PSCF), originally developed by Ashbaugh et al. (1985), which calculates the probability that a source is located at latitude *i* and longitude *j*. The basic assumption of PSCF is that if a source is located at a specific spot, an air parcel back trajectory passing over that location can collect the material from the source and transports it along the trajectory to the receptor site (Carslaw 2015).

Air parcel back trajectories ending at a receptor site are represented by segment endpoints. Each endpoint has three coordinates (latitude, longitude and height) representing the central location of an air parcel at a particular time. To calculate the PSCF, the whole geographic region covered by the trajectories is divided into an array of grid cells whose size is dependent on the geographical scale of the problem so that the PSCF will be a function of locations as defined by the cell indices *i* and *j*. Air parcel backward trajectories were related to the composition of measured concentrations by matching the time of arrival of each trajectory at the receptor site. PSCF values for each grid cell were calculated by counting the trajectory segment endpoints that terminate within the grid cells. The number of endpoints that fall in the ij^{th} cell is $n(i,j)$. The number of endpoints for the same cell when the corresponding samples show concentrations higher than a certain criterion value – by default the 90th percentile – is defined to be $m(i,j)$. The PSCF value for the ij^{th} cell is defined as (Hopke 2016):

$$PSCF(i,j) = \frac{m(i,j)}{n(i,j)}$$

Thus, the potential source contribution function can be interpreted as a conditional probability describing the spatial distribution of probable geographical source locations inferred by using trajectories arriving at the sampling site. Cells related to the high values of the potential source contribution function are the potential source areas (Polissar et al. 1999).

In the PSCF analysis, it is likely that the small values of $n(i,j)$ produce high $PSCF_{ij}$ values with high uncertainties. For large values of *n*, there is more statistical stability in the calculated value. In order to minimize this artefact, an empirical weight function $W(n_{ij})$ is multiplied into the PSCF value to better reflect the uncertainty in the values for these cells (Polissar et al. 1999):

$$W(n_{ij}) = \begin{cases} 1.00 & n_{ij} \geq 4 \\ 0.85 & n_{ij} = 3 \\ 0.65 & n_{ij} = 2 \\ 0.50 & n_{ij} = 1. \end{cases}$$

Although the trajectory segment endpoints are subject to uncertainty, a sufficient number of endpoints should provide accurate estimates of the source locations if the location errors are random and not systematic. Cells containing emission sources would be identified with conditional probabilities close to 1 assuming that trajectories that have crossed the cells effectively transport the emitted contaminant to the receptor site. The PSCF model thus provides a means to map the source potentials of geographical areas, though it does not apportion the contribution of the identified source area to the measured receptor data (Hopke 2016).

Calculated on basis of the previously described back trajectories together with the simultaneously measured de-seasonalised and de-trended CO_2 concentrations of the years 2000–2015 at the Schneefernerhaus, the PSCF-map of Fig. 5.2 refers to probable source regions especially Northeast of the receptor site (East of Germany and Poland), whereas the probability of emission sources within the central alpine region is zero even though this is the highest frequented area due to an alpine station as receptor site.

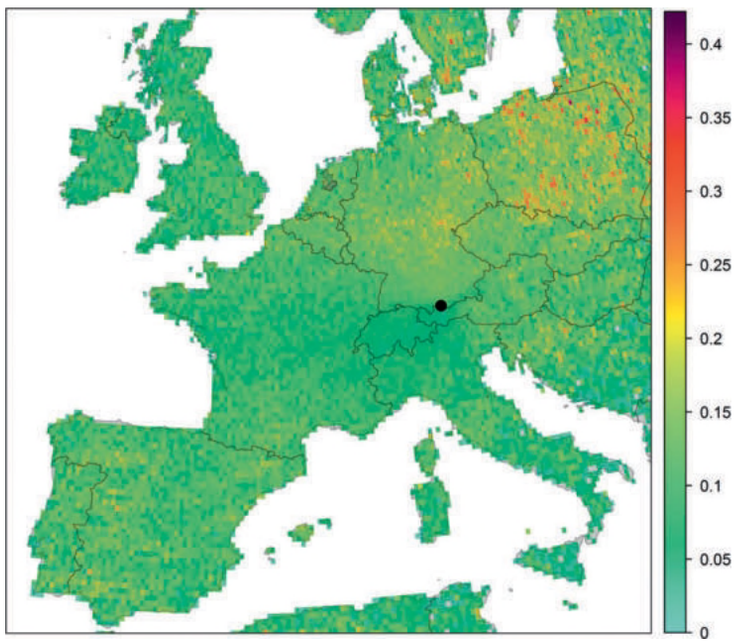

Fig. 5.2: Potential Source Contribution Function providing the probability (in %) that a source for high de-seasonalised and de-trended CO_2 concentrations (> 90th percentile) measured during the study period 2000–2015 at the receptor site Schneefernerhaus is located at the colour-coded grid cells of the map.

12.5.3 Concentration Weighted Trajectory fields (CWT)

A limitation of the PSCF method is that grid cells can have the same PSCF value when sample concentrations are either only slightly higher or much higher than the criterion (Hsu et al. 2003). As a result, it can be difficult to distinguish moderate sources from strong ones. Therefore, an advanced approach called the Concentration Weighted Trajectory fields (CWT) has been derived by Seibert et al. (1994) based on a grid domain as in the PSCF method. In analogue to the preceding PSCF, this second receptor modelling approach connects the on-site arriving paths of air masses to the contemporaneously measured short-term fluctuations in the CO_2 concentrations. In addition to the method of PSCF, however, the CWT approach also considers the residence time of the air parcels over geographic areas prior to their arrival at the observatory. Beyond that, the CWT methodology is able to distinguish between moderate sources/sinks and intense ones (Begum et al. 2005).

For CWT, a grid domain forms again the basis to identify contributing regions within the catchment area of the site. For each grid cell of the domain, Seibert et al. (1994) computed the mean concentration of the investigated species or chemical compound as follows:

$$\ln(\overline{C}_{ij}) = \frac{1}{\sum_{k=1}^{N} \tau_{ijk}} \sum_{k=1}^{N} \ln(c_k)\tau_{ijk}$$

where i and j are the indices of the grid, k the index of trajectory, N the total number of trajectories used in analysis, c_k the pollutant concentration measured upon arrival of trajectory k, and τ_{ijk} the residence time of trajectory k in grid cell (i, j). A high value of τ_{ij} means that air parcels passing over cell (i, j) would, on average, cause high concentrations at the receptor site and vice versa (Carslaw 2015).

All gridded receptor models based on air mass pathways are founded on the basic assumption that air parcel back trajectories crossing a grid cell (i, j) where a source or sink is located, transport the entailed alterations of the atmospheric trace gas concentration effectively to the receptor (Hopke, 2003). The grid cells are colour-coded according to their probability to act as emission sources or sinks and, taken in their entirety, constitute a complete map (Cheng et al. 2015).

These maps representing the relevant areas affecting the concentrations at the measuring site are quite reliable, as comparisons with known emitters have shown (Begum et al. 2005). For the receptor site Schneefernerhaus, CO_2 released from forest fires in the Mediterranean area during summer (especially during hot years, e.g. 2003) as well as wood and coal combustion during winter (particularly in cold years, e.g. 2005/2013) are recognised as major emitters for CO_2 (see Fig. 5.3).

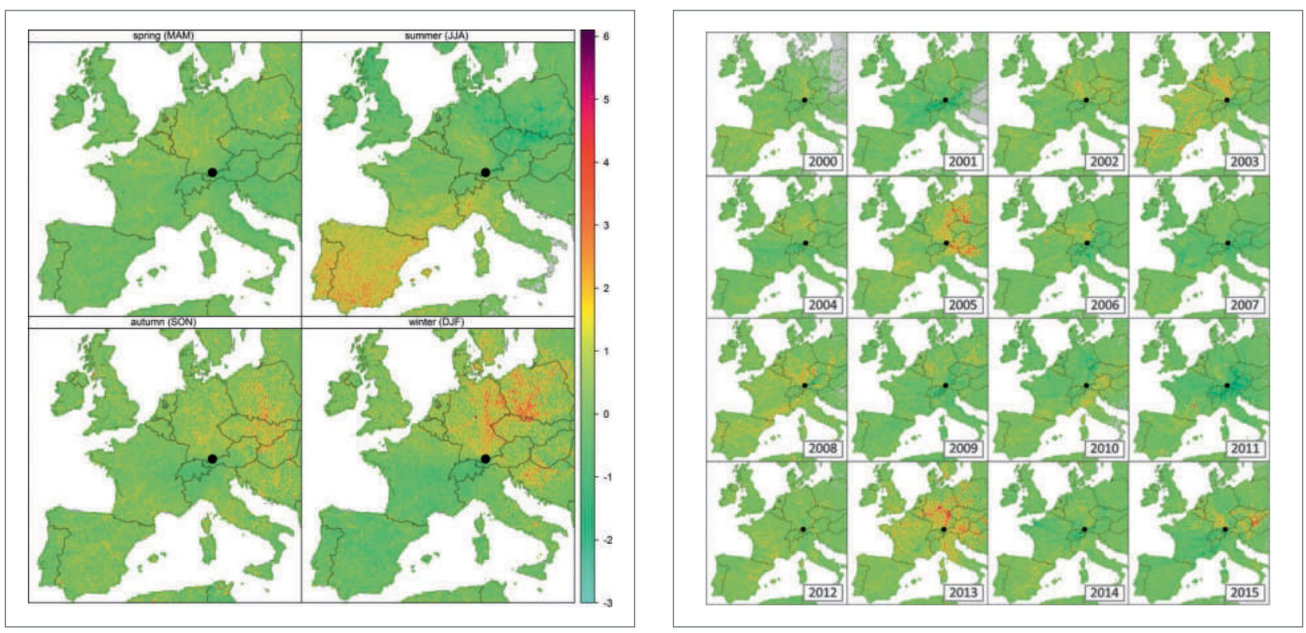

Fig. 5.3: Concentration Weighted Trajectory fields quantifying the influence of source and sink areas to the deviations of the de-seasonalised and de-trended CO_2 concentrations [in ppm] at the receptor site Schneefernerhaus, seasonally averaged (left) for the entire study period 2000–2015 and for individual years (right – same scale as the seasonal pendant).

References

Ashbaugh, L. L., Malm, W. C., Sadeh, W. Z. (1985): A residence time probability analysis of sulfur concentrations at Grand Canyon National Park. *Atmospheric Environment,* 19, 1263–1270.

Begum, B. A., Kim, E., Jeong, C.-H., Lee, D.-W., Hopke, P. K. (2005): Evaluation of the potential source contribution function using the 2002 Quebec forest fire episode. *Atmospheric Environment,* 39, 3719–3724.

Carslaw, D. C. (2015): The openair manual – open-source tools for analyzing air pollution data. Manual for version 1.1–4., King's College London. 287 p.

Cheng, I., Xu, X., Zhang, L. (2015): Overview of receptor-based source apportionment studies for speciated atmospheric mercury. *Atmospheric Chemistry and Physics,* 15, 7877–7895.

Crawford, J., Zahorowski, W., Cohen, D. D. (2009): A new metric space incorporating radon-222 for generation of back trajectory clusters in atmospheric pollution studies. *Atmospheric Environment*, 43, 371–381.

Fleming, Z. L., Monks, P. S., Manning, A. J. (2012): Review: Untangling the influence of air-mass history in interpreting observed atmospheric composition. *Atmospheric Research*, 104–105, 1–39.

Hopke, P., K. (2003): Recent developments in receptor modeling. *Journal of Chemometrics*, 17, 255–265.

Hopke, P. K. (2016): Review of receptor modeling methods for source apportionment. *Journal of the Air & Waste Management Association*, 66, 237–259.

Hsu, Y. K., Holsen, T. M., Hopke, P. K. (2003): Comparison of hybrid receptor models to locate PCB sources in Chicago. *Atmospheric Environment*, 37, 545–562.

Polissar, A. V., Hopke, P. K., Paatero, P., Kaufmann, Y. J., Hall, D. K., Bodhaine, B. A., Dutton, E. G., Harris, J. M. (1999): The aerosol at Barrow, Alaska: long-term trends and source locations. *Atmospheric Environment*, 33, 2441–2458.

Seibert, P., Kromp-Kolb, H., Baltensperger, U., Jost, D. (1994): Trajectory analysis of high-alpine air pollution data. In: Gryning, S.-E., Millán M. M. (eds): *Air Pollution Modeling and Its Application X. NATO – Challenges of Modern Society*, 18, 595–596.

Seinfeld, J.H. & Pandis S.N. (2016): Atmospheric Chemistry and Physics – From Air Pollution to Climate Change. 3. Ed., Wiley, 1152 p.

Stohl, A., Eckhardt, S., Forster, C., James, P., Spichtinger, N., Seibert, P. (2002): A replacement for simple back trajectory calculations in the interpretation of atmospheric trace substance measurements. *Atmospheric Environment*, 36, 4635–4648.

Stohl, A., Forster, C., Frank, A., Seibert, P., Wotawa, G. (2005): Technical note – The Lagrangian particle dispersion model FLEXPART version 6.2, *Atmospheric Chemistry and Physics,* 5, 2461–2474.